

TECHNICAL NOTES
NATIONAL ADVISORY COMMITTEE FOR AERONAUTICS

No. 581

A STUDY OF AUTOGIRO ROTOR-BLADE OSCILLATIONS
IN THE PLANE OF THE ROTOR DISK

By John B. Wheatley
Langley Memorial Aeronautical Laboratory

NATIONAL ADVISORY COMMITTEE FOR AERONAUTICS
LANGLEY MEMORIAL AERONAUTICAL LABORATORY
LANGLEY FIELD, VIRGINIA

RETURN

REQUESTS FOR INFORMATION SHOULD BE ADDRESSED
AS FOLLOWS:

NATIONAL ADVISORY COMMITTEE FOR AERONAUTICS
1724 F STREET, N.W.
WASHINGTON 25, D.C.

Washington
September 1936

NACA LIBRARY
LANGLEY MEMORIAL AERONAUTICAL
LABORATORY
Langley Field, Va.

NATIONAL ADVISORY COMMITTEE FOR AERONAUTICS

TECHNICAL NOTE NO. 581

A STUDY OF AUTOGIRO ROTOR-BLADE OSCILLATIONS
IN THE PLANE OF THE ROTOR DISK

By John B. Wheatley

SUMMARY

An analysis of the factors governing the oscillation of an autogiro rotor blade in the plane of the rotor disk showed that the contribution of the air forces to the resultant motion was small and that the oscillation is essentially a direct effect of the rotor-blade flapping motion. A comparison of calculated oscillations with those measured in flight on three different rotors disclosed that the calculations gave satisfactory agreement with experiment. The calculated air forces on the rotor blade appear to be larger than the experimental ones, but this discrepancy can be attributed to the deficiencies in the strip analysis.

INTRODUCTION

An autogiro rotor blade is connected to the rotor hub in such a way as to permit two articulations, one about the horizontal hinge and one about the vertical hinge. The horizontal hinge axis is perpendicular to the blade span axis and to the rotor axis and permits the blade to oscillate freely in a plane containing the blade span axis and the rotor axis. The vertical hinge axis is parallel to and offset from the rotor axis and permits the blade to oscillate in the plane of rotation. This articulation is required because the forces acting on the blade in the rotor disk are of an unsteady nature and experience has shown that heavy stresses and uncomfortable vibrations arise if this articulation is not used. In addition, motion about this hinge is damped by friction so that transient vibrations will quickly subside.

A knowledge of the motion about the vertical hinge is of value for several reasons. The nature of the oscilla-

tion must be known in order to determine intelligently the amount of damping required by the blade. In addition, a verified analysis of this oscillation suggests the possibility of subjecting all rotor characteristics to some form of mathematical analysis and lessens the dependence of the designer upon empirical rules. This paper presents an analysis of this phase of the blade motion and shows a comparison between calculated and measured results which supports the validity of the analysis.

ANALYSIS

The autogiro rotor-blade oscillations in the plane of the rotor disk will be divided into two parts: First, the motion about the vertical pin that arises from the consideration of the changing moment of inertia of the blades about the axis of rotation caused by the flapping motion; and second, the forced vibration of the blades about the vertical hinge caused by the variation of the air torque from a mean value of zero. This method of considering the blade motion requires some justification, because it is not obvious that the two oscillations mentioned are independent of each other.

The experimental study of vertical-hinge oscillations made with a motion-picture camera on the rotor hub established that the amplitude of the oscillation was less than 0.015 radian and that the oscillation consisted mainly of a fundamental of the same frequency as the rotor revolutions. The angular velocity of this oscillation is consequently less than 0.015 times the mean angular velocity of the rotor; therefore the peripheral velocity added by the oscillation can safely be neglected. This condition justifies the assumption that the air forces tending to oscillate the blade may be considered independent of this oscillation. In addition, the amplitude of the oscillation is small enough to justify the assumption that the moment of inertia of the blade is not appreciably changed by the oscillation; the effect of the changing moment of inertia can, therefore, also be considered independent of the vertical-hinge oscillation.

Before the analysis is carried further, it is pertinent to consider briefly the problem of hub vibrations. If the blade oscillation about the vertical pin included a harmonic of the same order as the number of blades, the

forces arising from the oscillation that acts on the hub would add and the motion of the hub would be affected. It can be shown that the sum of the individual effects is zero for all harmonics except the one mentioned. It has been experimentally verified that the third and higher order harmonics are negligible. In addition, experimental observations indicate that the hub motion is steady, inasmuch as no steady vibrations in the readings of a sensitive tachometer were noted. It consequently can be assumed that the hub does not oscillate but rotates at a constant velocity.

Let I be the instantaneous moment of inertia of a rotor blade and let I_0 be the moment of inertia when the angle of flapping β (about the horizontal pin) is zero. Then

$$I = I_0 \cos^2 \beta \quad (1)$$

The assumption that $\sin \beta = \beta$ is justified by the small range covered by β (less than 15°). Then

$$I = I_0 (1 - \sin^2 \beta) = I_0 (1 - \beta^2) \quad (2)$$

Let Ω_i be the instantaneous blade angular velocity. The law of constant angular momentum states that

$$I \Omega_i = K \quad (3)$$

or

$$\Omega_i = \frac{K}{I} = \frac{K}{I_0} (1 + \beta^2) \quad (4)$$

where β^4 and higher powers are neglected because β is small. From reference 1,

$$\beta = a_0 - a_1 \cos \psi - b_1 \sin \psi - a_2 \cos 2\psi - b_2 \sin 2\psi \quad (5)$$

Finally

$$\begin{aligned} \Omega_1 = \frac{K}{I_0} & \left[1 + a_0^2 + \frac{1}{2} a_1^2 + \frac{1}{2} b_1^2 + \frac{1}{2} a_2^2 + \frac{1}{2} b_2^2 \right. \\ & - (2a_0a_1 - a_1a_2 - b_1b_2) \cos \psi - (2a_0b_1 - a_1b_2 + b_1a_2) \sin \psi \\ & - (2a_0a_2 - \frac{1}{2} a_1^2 + \frac{1}{2} b_1^2) \cos 2\psi - (2a_0b_2 - a_1b_1) \sin 2\psi \\ & \left. - (-a_1a_2 + b_1b_2) \cos 3\psi - (-a_1b_2 - b_1a_2) \sin 3\psi \right] \quad (6) \end{aligned}$$

Integrating to obtain a displacement equation and letting the mean $\Omega_1 = \Omega$

$$\begin{aligned} \int_0^t \Omega_1 dt = \psi_1 = \frac{K}{I_0} & \left[(1 + a_0^2 + \frac{1}{2} a_1^2 + \frac{1}{2} b_1^2 + \frac{1}{2} a_2^2 + \frac{1}{2} b_2^2) t \right. \\ & + \frac{1}{\Omega} (2a_0b_1 - a_1b_2 + b_1a_2) \cos \psi - \frac{1}{\Omega} (2a_0a_1 - a_1a_2 - b_1b_2) \sin \psi \\ & + \frac{1}{2\Omega} (2a_0b_2 - a_1b_1) \cos 2\psi - \frac{1}{2\Omega} (2a_0a_2 - \frac{1}{2} a_1^2 + \frac{1}{2} b_1^2) \sin 2\psi \\ & \left. - \frac{1}{3\Omega} (a_1b_2 + b_1a_2) \cos 3\psi + \frac{1}{3\Omega} (a_1a_2 - b_1b_2) \sin 3\psi \right] \quad (7) \end{aligned}$$

The part of equation (7), varying with ψ which expresses the component ζ_1 of the angular displacement of the blade oscillation, can be more briefly written as

$$\begin{aligned} \zeta_1 = u_1 \cos \psi + v_1 \sin \psi + \frac{1}{2} u_2 \cos 2\psi + \frac{1}{2} v_2 \sin 2\psi \\ + \frac{1}{3} u_3 \cos 3\psi + \frac{1}{3} v_3 \sin 3\psi \quad (8) \end{aligned}$$

where

$$u_1 = 2 a_0 b_1 - a_1 b_2 + b_1 a_2, \quad v_1 = -2 a_0 a_1 + a_1 a_2 + b_1 b_2,$$

$$u_2 = 2 a_0 b_2 - a_1 b_1, \text{ etc.}$$

since

$$\frac{K}{I_0 \Omega} = 1$$

The instantaneous air torque acting on a blade can be derived from equation (10-1) of reference 1

$$Q = \int_0^{BR} \frac{1}{2} \rho c U^2 \varphi C_L r dr - \int_0^R \frac{1}{2} \rho c U^2 \delta r dr \quad (9)$$

The deficiencies in this expression arise from the assumptions upon which it is based. The more important ones are: First, that the lift coefficient is proportional to the angle of attack and has no maximum value; second, that the angle φ , the angle of the local velocity to the plane of the rotor disk, is everywhere small enough to equate the sine to the angle; third, an average value δ of the blade profile-drag coefficient is employed which renders somewhat uncertain the calculation of instantaneous values of the profile-drag torque; fourth, the lift torque is expressed incorrectly where the tangential velocity Ωr is less than the forward velocity V ; and fifth, the induced downward velocity is assumed constant over the disk for simplicity, which again renders the derived instantaneous values uncertain. The equation is, however, the only available means of attacking the problem and will consequently be used, though with caution.

The solution Q_ψ is obtained by substituting for U , φ and C_L as in reference 1, and an expression of the following type is derived:

$$Q_\psi = \frac{1}{2} \rho c a \Omega^2 R^4 (A_1 \cos \psi + B_1 \sin \psi + A_2 \cos 2\psi + B_2 \sin 2\psi + A_3 \cos 3\psi + B_3 \sin 3\psi + \dots) \quad (10)$$

The coefficients A_n and B_n are functions of μ , θ , λ , a_n , and b_n and are derived in the appendix. The notation Q_ψ indicates that only the torque varying with ψ is retained, since by hypothesis

$$\int_0^{2\pi} Q \, d\psi = 0$$

The component of the angular displacement of the blade arising from Q_ψ is designated ξ_a . If R_v is the radius of the vertical pin, r the radius of the blade element dr , m_x the line density of the blade, R the tip radius, and Q_R the restoring couple arising from ξ_a , then

$$Q_R = \int_{R_v}^R m_x \Omega^2 R_v r \xi \, dr \quad (11)$$

The angle ξ is diagrammed in figure 1. By reference to this figure and the law of sines, assuming small angles,

$$\xi = \xi_a \frac{r - R_v}{r} \quad (12)$$

and

$$Q_R = \int_{R_v}^R m_x \Omega^2 (r - R_v) R_v \xi_a \, dr \quad (13)$$

It is evident that $\int_{R_v}^R m_x (r - R_v) \, dr$ integrates into the mass moment M_m of the blade about the vertical pin - then

$$Q_R = M_m \Omega^2 R_v \xi_a \quad (14)$$

The equation of motion of the blade can now be written

$$I_v \frac{d^2 \xi_a}{dt^2} + M_m \Omega^2 R_v \xi_a = Q_\psi \quad (15)$$

where I_v is the moment of inertia of the blade about the vertical pin.

No damping term is included because damping of any

reasonable magnitude will have a negligible effect on the frequency and amplitude of the steady forced vibration.

Equation (15) is a well-known form of differential equation, the solution of which can be obtained directly by assuming

$$\zeta_2 = C_1 \cos \psi + D_1 \sin \psi + C_2 \cos 2\psi + D_2 \sin 2\psi \\ + C_3 \cos 3\psi + D_3 \sin 3\psi \quad (16)$$

The C and D coefficients are found by substituting for ζ_2 from equation (16) in equation (15) and equating the coefficients of trigonometric functions. It is then found that

$$C_1 = \frac{\frac{1}{2} \rho c a R^4 A_1}{M_m R_v - I_0} \quad (17)$$

$$D_1 = \frac{\frac{1}{2} \rho c a R^4 B_1}{M_m R_v - I_0} \quad (18)$$

$$C_2 = \frac{\frac{1}{2} \rho c a R^4 A_2}{M_m R_v - 4I_0} \quad (19)$$

$$D_2 = \frac{\frac{1}{2} \rho c a R^4 B_2}{M_m R_v - 4I_0} \quad (20)$$

$$C_3 = \frac{\frac{1}{2} \rho c a R^4 A_3}{M_m R_v - 9I_0} \quad (21)$$

$$D_3 = \frac{\frac{1}{2} \rho c a R^4 B_3}{M_m R_v - 9I_0} \quad (22)$$

The resultant blade displacement ζ can now be obtained by adding equation (16) to equation (8), neglecting all constant terms, then

$$\zeta = E_1 \cos \psi + F_1 \sin \psi + E_2 \cos 2\psi + F_2 \sin 2\psi \\ + E_3 \cos 3\psi + F_3 \sin 3\psi \quad (23)$$

where

$$\left. \begin{aligned} E_1 &= C_1 + v_1 \\ F_1 &= D_1 + u_1 \\ E_2 &= C_2 + \frac{1}{2} v_2 \\ F_2 &= D_2 + \frac{1}{2} u_2 \\ E_3 &= C_3 + \frac{1}{3} v_3 \\ F_3 &= D_3 + \frac{1}{3} u_3 \end{aligned} \right\} \quad (24)$$

It is of interest to consider a simplified solution in which the C and D coefficients are neglected and a flapping curve is assumed that has no second harmonics. Then

$$\beta = a_0 - a_1 \cos \psi - b_1 \sin \psi \quad (25)$$

$$\beta_{\max} = a_0 + \sqrt{a_1^2 + b_1^2} \quad (26)$$

$$\begin{aligned} \zeta &= 2 a_0 b_1 \cos \psi - 2 a_0 a_1 \sin \psi - \frac{1}{2} a_1 b_1 \cos 2 \psi \\ &+ \left(\frac{1}{2} a_1^2 - \frac{1}{2} b_1^2 \right) \sin 2 \psi \end{aligned} \quad (27)$$

The maximum value of ζ is, neglecting the second harmonics, which are normally quite small:

$$\zeta_{\max} = 2 a_0 \sqrt{a_1^2 + b_1^2} = 2 a_0 (\beta_{\max} - a_0) \quad (28)$$

TESTS AND APPARATUS

The rotor-blade motions about the horizontal and vertical pins of several autogiros were measured by mounting a motion-picture camera on the rotor hub and photographing the rotor blade in flight (reference 2). Data simultaneously obtained determined the tip-speed ratios. One rotor, the PCA-2, was also tested alone in the full-scale wind tunnel (reference 3), the tests affording some necessary data shown in subsequent tables. The physical characteristics of the three rotors tested, the PCA-2, the PAA-1, and the KD-1, are given in tables I, II, and III, respectively.

RESULTS

The flapping coefficients of the PCA-2 rotor are pre-

sented as functions of the tip-speed ratio in figure 2. Figures 3, 4, and 5 present comparisons of the experimental vertical-pin oscillation in coefficient form with values calculated from the air forces alone, the angular momentum alone, and the combined air forces and angular momentum, respectively. No third harmonics are given since both calculated and experimental values were found to be negligible. A comparison of the vertical-pin motion during a rotor revolution at a tip-speed ratio of 0.5, based on calculated and experimental results, is shown in figure 6.

The experimental flapping coefficients of the PAA-1 rotor are presented in figure 7 as functions of the tip-speed ratio. The coefficients of the vertical-pin oscillation of this rotor based on experiment and upon calculation from the angular-momentum law are given in figure 8.

Figure 9 shows the experimental flapping coefficients of the KD-1 rotor as a function of tip-speed ratio. The experimental coefficients of the vertical-pin oscillation of this rotor are compared in figure 10 with the coefficients calculated from the angular momentum alone.

All calculations are based upon the data in tables I, II, and III and in figures 2, 7, and 9, which show the experimental blade flapping-motion data for each rotor.

DISCUSSION

In order that the designer be able to calculate the rotor-blade motion about the vertical pin, he must first calculate the flapping motion about the horizontal pin. This problem has been analyzed and discussed in reference 1 and will not be touched upon here.

The most important deduction in this study is arrived at from an examination of figures 3, 4, and 5, which demonstrate that the blade motion about the vertical pin arising from the air forces is negligible compared with the motion caused by the angular momentum. In addition, figures 4, 8, and 10 indicate that a reasonably accurate calculation of the blade motion can be made without considering the air forces.

The agreement between the calculated and experimental blade-motion coefficients is individually excellent as shown in figures 4, 8, and 10, except for the component u_1 , the $\sin \psi$ term. The poor agreement between this calculated

factor and the measured one can be explained by figure 3. The factor D_1 represents the calculated $\sin \psi$ component arising from the air forces. It appears that the influence of the air forces on the motion is reflected almost entirely in the coefficient of $\sin \psi$ and that the D_1 term representing this effect is of the proper sign to make u_1 agree more closely with experiment. It is found, however, in figure 5 that F_1 , which is the sum of u_1 and D_1 , disagrees with the experiment as radically as does u_1 . It must therefore be concluded that the calculation has overestimated the magnitude of D_1 . This deduction is reasonable because the actual accelerating torque on the retreating side of the disk must be less than the calculated torque because the strip analysis assumes a constant lift-curve slope and does not take into account the existence of a maximum lift; both of these factors would cause an over-estimation of the accelerating torque where the local angles of attack are large.

The plotted blade motion in figure 6 illustrates graphically the error in the motion arising from the u_1 term; if this calculated term agreed with the experiment the two curves of figure 6 would, for all practical purposes, coincide.

An examination of figures 4, 8, and 10 suggests that a very close approximation to the actual motion about the vertical pin can be obtained by calculating the motion from the angular momentum alone and arbitrarily adding to the u_1 term a correction factor of the magnitude indicated in these figures.

CONCLUSIONS

1. The autogiro rotor-blade oscillation about the vertical pin is essentially a direct effect of the rotor-blade flapping motion.
2. The effect of the air forces on the autogiro rotor-blade oscillation about the vertical pin was shown by both calculation and experiment to be of second order in comparison to the effect of the blade flapping.
3. The deficiencies of the strip analysis result in the overestimation of the air forces acting on the rotor blades.

Langley Memorial Aeronautical Laboratory,
National Advisory Committee for Aeronautics,
Langley Field, Va., June 23, 1936.

APPENDIX

From reference 1, equation (10-1),

$$Q = \int_0^{BR} \frac{1}{2} \rho c U^2 \varphi C_L r dr - \int_0^R \frac{1}{2} \rho c U^2 \delta r dr$$

Substitute for U , φ and C_L as in reference 1; integrate, then, dropping all constant terms that must sum to zero since the mean rotor angular velocity is constant,

$$\begin{aligned} Q_\psi = & \frac{1}{2} \rho c a \Omega^2 R^4 \left\{ \left(-\mu a_0 \left[\frac{1}{3} \theta_0 B^3 + \frac{1}{4} \theta_1 B^4 \right] + b_1 \left[\frac{1}{4} \theta_0 B^4 + \frac{1}{5} \theta_1 B^5 \right] \right. \right. \\ & + \frac{1}{4} \mu^2 b_1 \left[\frac{1}{2} \theta_0 B^2 + \frac{1}{3} \theta_1 B^3 \right] - \frac{1}{2} \mu a_2 \left[\frac{1}{3} \theta_0 B^3 + \frac{1}{4} \theta_1 B^4 \right] \\ & - \mu \lambda a_0 B^2 + \frac{2}{3} \lambda b_1 B^3 + \frac{1}{2} \mu \lambda a_2 B^2 - \frac{2}{3} \mu a_0 b_2 B^3 \\ & \left. \left. - \frac{3}{4} \mu^2 a_0 a_1 B^2 + \frac{1}{3} \mu a_1 b_1 B^3 + \frac{1}{2} a_1 a_2 B^4 + \frac{1}{2} b_1 b_2 B^4 \right) \cos \psi \right. \\ & + \left(\mu \lambda \left[\frac{1}{2} \theta_0 B^2 + \frac{1}{3} \theta_1 B^3 \right] - a_1 \left[\frac{1}{4} \theta_0 B^4 + \frac{1}{5} \theta_1 B^5 \right] + \frac{1}{4} \mu^2 a_1 \left[\frac{1}{2} \theta_0 B^2 + \frac{1}{3} \theta_1 B^3 \right] \right. \\ & - \frac{1}{2} \mu b_2 \left[\frac{1}{3} \theta_0 B^3 + \frac{1}{4} \theta_1 B^4 \right] - \frac{2}{3} \lambda a_1 B^3 + \frac{1}{2} \mu \lambda b_2 B^2 - \frac{1}{4} \mu^2 a_0 b_1 B^2 \\ & + \frac{2}{3} \mu a_0 a_2 B^3 - \frac{1}{6} \mu a_1^2 B^3 + \frac{1}{2} a_1 b_2 B^4 + \frac{1}{6} \mu b_1^2 B^3 - \frac{1}{2} b_1 a_2 B^4 - \frac{2}{3} \mu \frac{\delta}{a} \left. \right) \sin \psi \\ & + \left(\mu a_1 \left[\frac{1}{3} \theta_0 B^3 + \frac{1}{4} \theta_1 B^4 \right] + 2 b_2 \left[\frac{1}{4} \theta_0 B^4 + \frac{1}{5} \theta_1 B^5 \right] + \frac{1}{2} \mu \lambda a_1 B^2 \right. \\ & + \frac{4}{3} \lambda b_2 B^3 + \frac{1}{4} \mu^2 a_0^2 B^2 - \frac{1}{3} \mu a_0 b_1 B^3 - \frac{1}{2} \mu^2 a_0 a_2 B^2 - \frac{1}{8} a_1^2 B^4 \\ & \left. \left. + \frac{1}{4} \mu^2 a_1^2 B^2 + \frac{2}{3} \mu a_1 b_2 B^3 + \frac{1}{8} b_1^2 B^4 + \frac{1}{3} \mu b_1 a_2 B^3 + \frac{1}{4} \mu^2 \frac{\delta}{a} \right) \cos 2\psi \right. \\ & + \left(-\frac{1}{2} \mu \lambda a_0 \left[\frac{1}{2} \theta_0 B^2 + \frac{1}{3} \theta_1 B^3 \right] + \mu b_1 \left[\frac{1}{3} \theta_0 B^3 + \frac{1}{4} \theta_1 B^4 \right] - 2 a_2 \left[\frac{1}{4} \theta_0 B^4 + \frac{1}{5} \theta_1 B^5 \right] \right. \\ & \left. + \frac{1}{2} \mu \lambda b_1 B^2 - \frac{4}{3} \lambda a_2 B^3 + \frac{1}{3} \mu a_0 a_1 B^3 - \frac{1}{2} \mu^2 a_0 b_2 B^2 \right. \end{aligned}$$

$$\begin{aligned}
& - \frac{1}{4} a_1 b_1 B^4 + \frac{1}{4} \mu^2 a_1 b_1 B^2 - \frac{2}{3} \mu a_1 a_2 B^3 + \frac{1}{3} \mu b_1 b_2 B^3 \Big) \sin 2\psi \\
& + \left(\frac{1}{4} \mu \lambda a_2 B^2 - \frac{1}{4} \mu^2 b_1 \left[\frac{1}{2} \theta_0 B^2 + \frac{1}{3} \theta_1 B^3 \right] + \frac{3}{2} \mu a_2 \left[\frac{1}{3} \theta_0 B^3 + \frac{1}{4} \theta_1 B^4 \right] \right. \\
& - \frac{1}{8} \mu^2 a_0 a_1 B^2 - \frac{1}{3} \mu a_0 b_2 B^3 + \frac{1}{6} \mu a_1 b_1 B^3 - \frac{1}{4} a_1 a_2 B^4 + \frac{1}{4} b_1 b_2 B^4 \Big) \cos 3\psi \\
& + \left(\frac{1}{4} \mu \lambda b_2 B^2 + \frac{1}{4} \mu^2 a_1 \left[\frac{1}{2} \theta_0 B^2 + \frac{1}{3} \theta_1 B^3 \right] + \frac{3}{2} \mu b_2 \left[\frac{1}{3} \theta_0 B^3 + \frac{1}{4} \theta_1 B^4 \right] \right. \\
& - \frac{1}{8} \mu^2 a_0 b_1 B^2 + \frac{1}{3} \mu a_0 a_2 B^3 - \frac{1}{12} \mu a_1^2 B^3 - \frac{1}{4} a_1 b_2 B^4 \\
& \left. + \frac{1}{12} \mu b_1^2 B^3 - \frac{1}{4} b_1 a_2 B^4 \right) \sin 3\psi \Big\}
\end{aligned}$$

REFERENCES

1. Wheatley, John B.: An Aerodynamic Analysis of the Autogiro Rotor with a Comparison between Calculated and Experimental Results. T.R. No. 487, N.A.C.A., 1934.
2. Wheatley, John B.: Wing Pressure Distribution and Rotor-Blade Motion of an Autogiro as Determined in Flight. T.R. No. 475, N.A.C.A., 1933.
3. Wheatley, John B., and Hood, Manley J.: Full-Scale Wind-Tunnel Tests of a PCA-2 Autogiro Rotor. T.R. No. 515, N.A.C.A., 1935.

TABLE I. PCA-2 Rotor Characteristics

Radius R, ft.	22.5
Moment of inertia about vertical pin I_1 , slug-ft. ²	316
Radius of vertical pin R_v , ft.646
Blade mass m, slugs	2.588
Blade chord (outer part of blade) c, ft.	1.833
Lift-curve slope a	5.85
Blade span efficiency factor B959
Blade pitch angle θ , radians	$-0.0157 + 0.0872 \frac{R}{R_1}$

(The values of λ and δ/a are calculated from reference 3)

μ	0.15	0.20	0.25	0.30	0.35	0.40	0.45	0.50	0.55	0.60	0.65	0.70
λ	0.0198	0.0185	0.0152	0.0114	0.0078	0.0045	0.0014	-0.0012	-0.0030	-0.0041	-0.0048	-0.0051
$\frac{\delta}{a}$.00172	.00171	.00178	.00190	.00200	.00215	.00226	.00239	.00255	.00270	.00284	.00299

TABLE II. PAA-1 Rotor Characteristics

Radius R , ft.	19
Estimated moment of inertia about vertical pin I_1 , slug-ft. ²	150
Estimated radius of vertical pin R_v , ft.	0.75
Blade mass m , slugs	1.65

TABLE III. KD-1 Rotor Characteristics

Radius R , ft.	20
Estimated moment of inertia about vertical pin I_1 , slug-ft. ²	155
Estimated radius of vertical pin R_v , ft.	0.792
Blade mass m , slugs	1.61

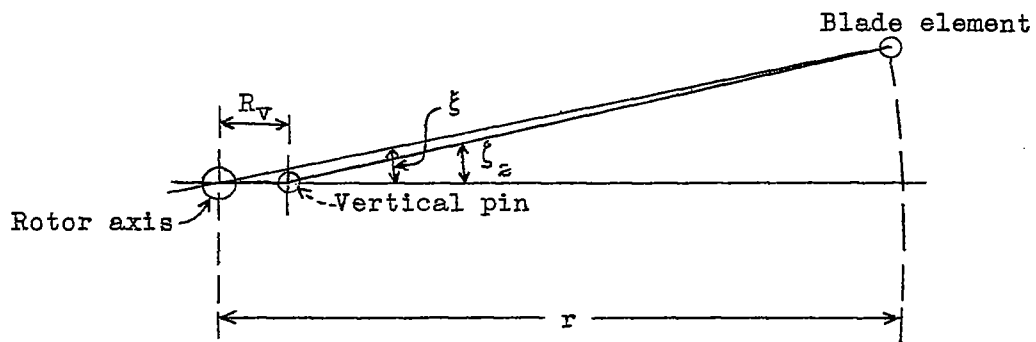


Figure 1.- Geometry of autogiro rotor blade and vertical-pin articulation.

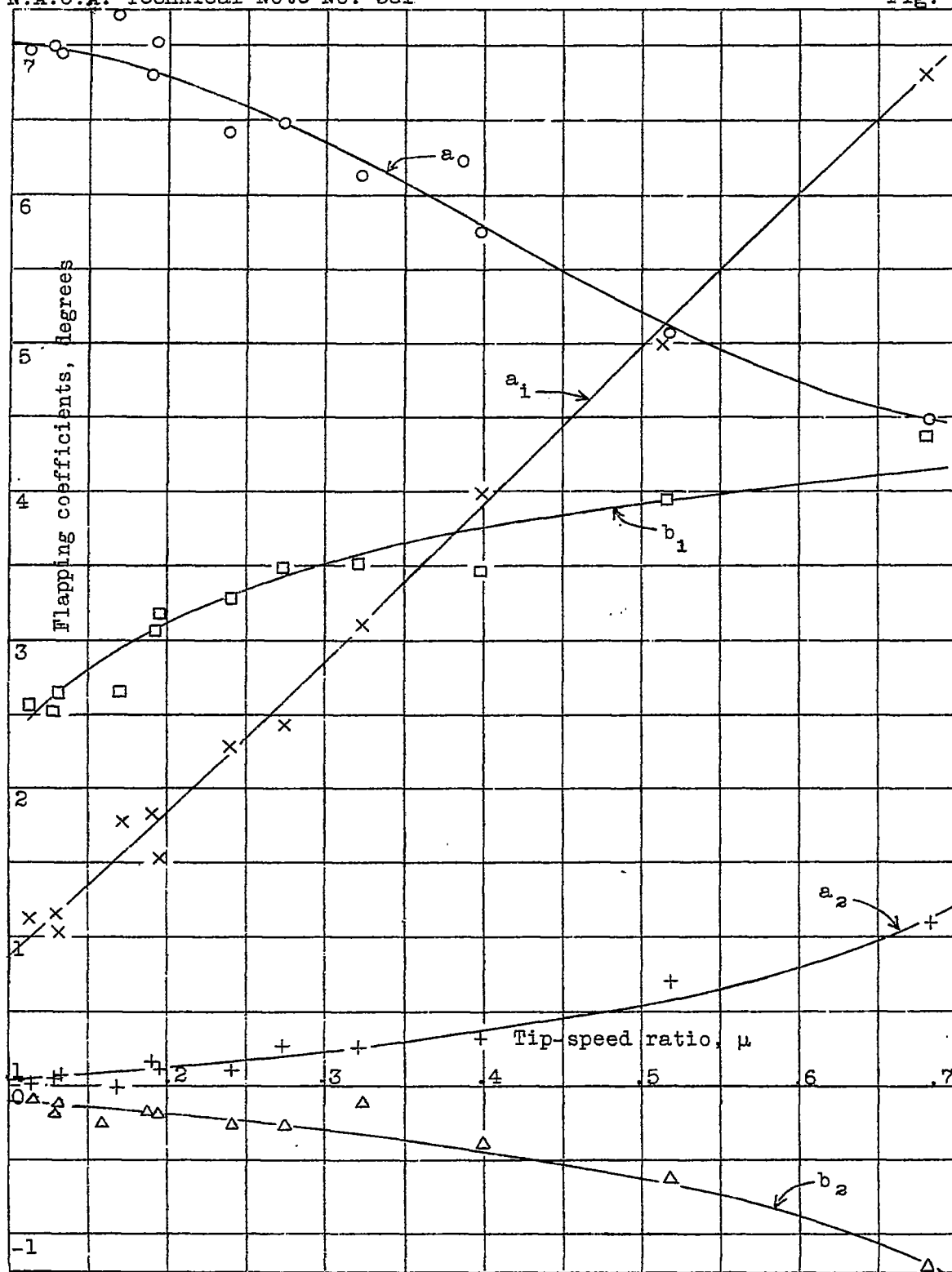


Figure 2.- Flapping coefficients of PCA-2 autogiro rotor as measured in flight.

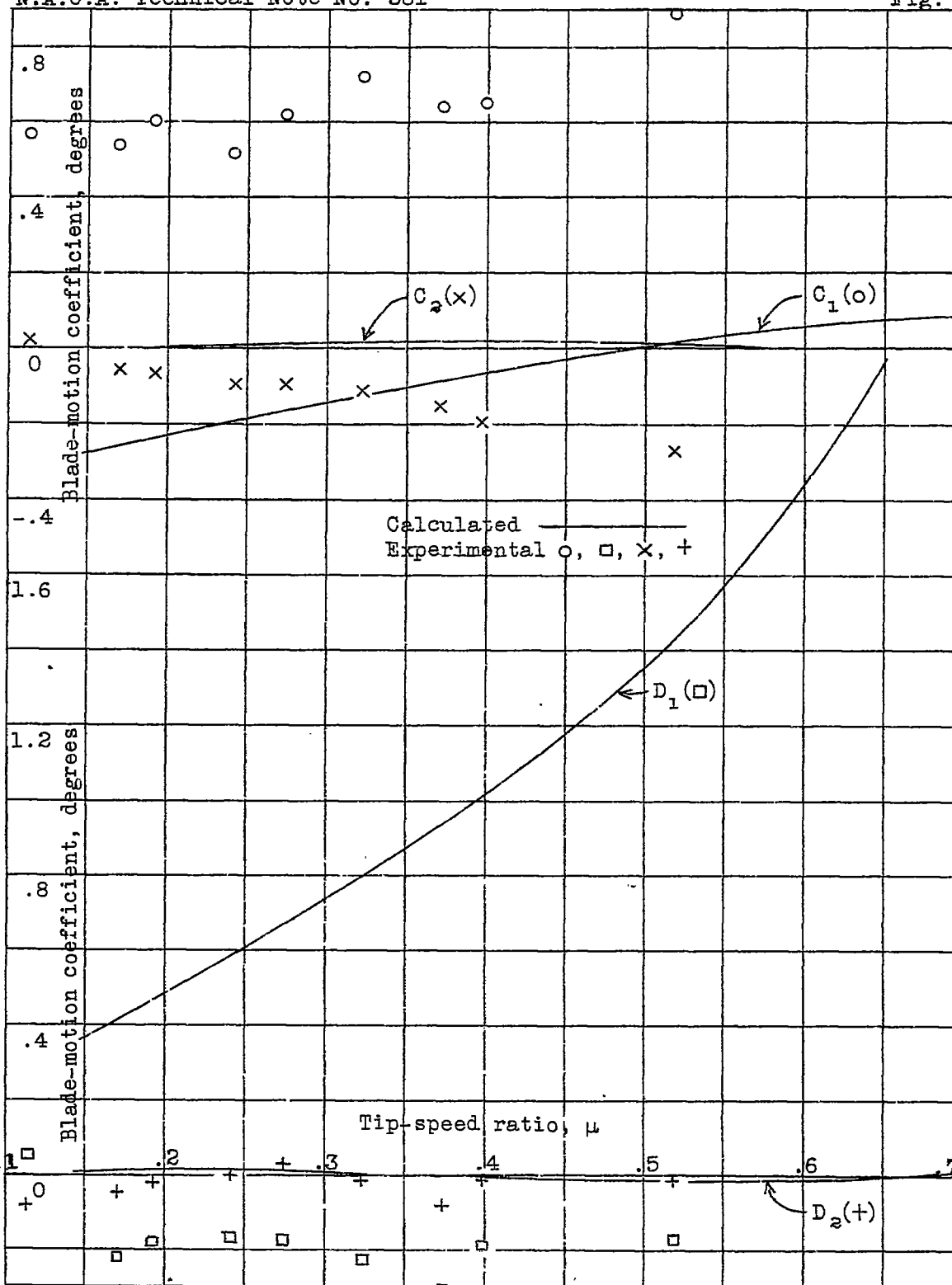


Figure 3.- Coefficients of PCA-2 rotor-blade motion about the vertical pin as measured in flight and as calculated from the air forces alone.

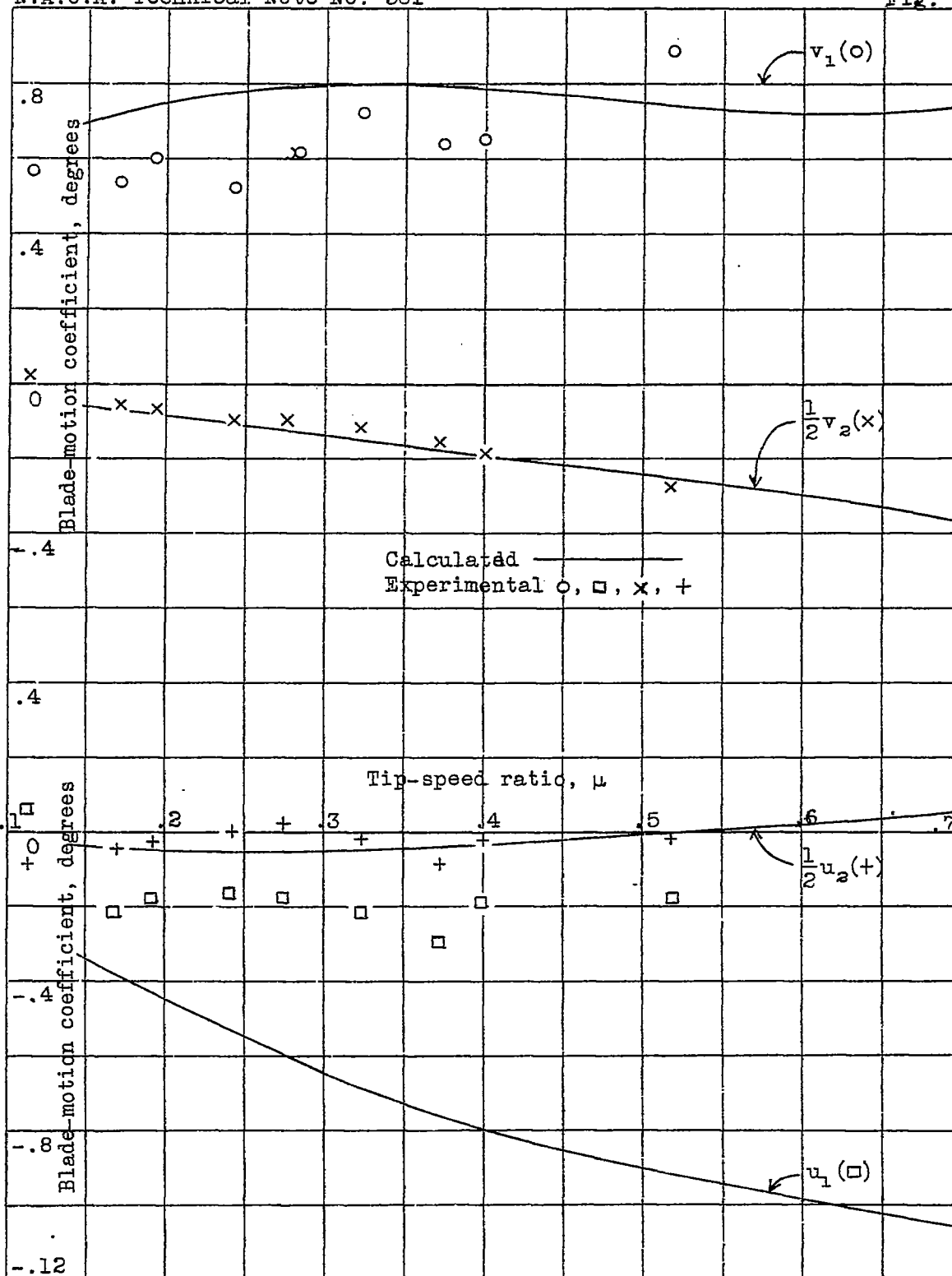


Figure 4.- Coefficients of PCA-2 rotor-blade motion about the vertical pin as measured in flight and as calculated from the angular momentum alone.

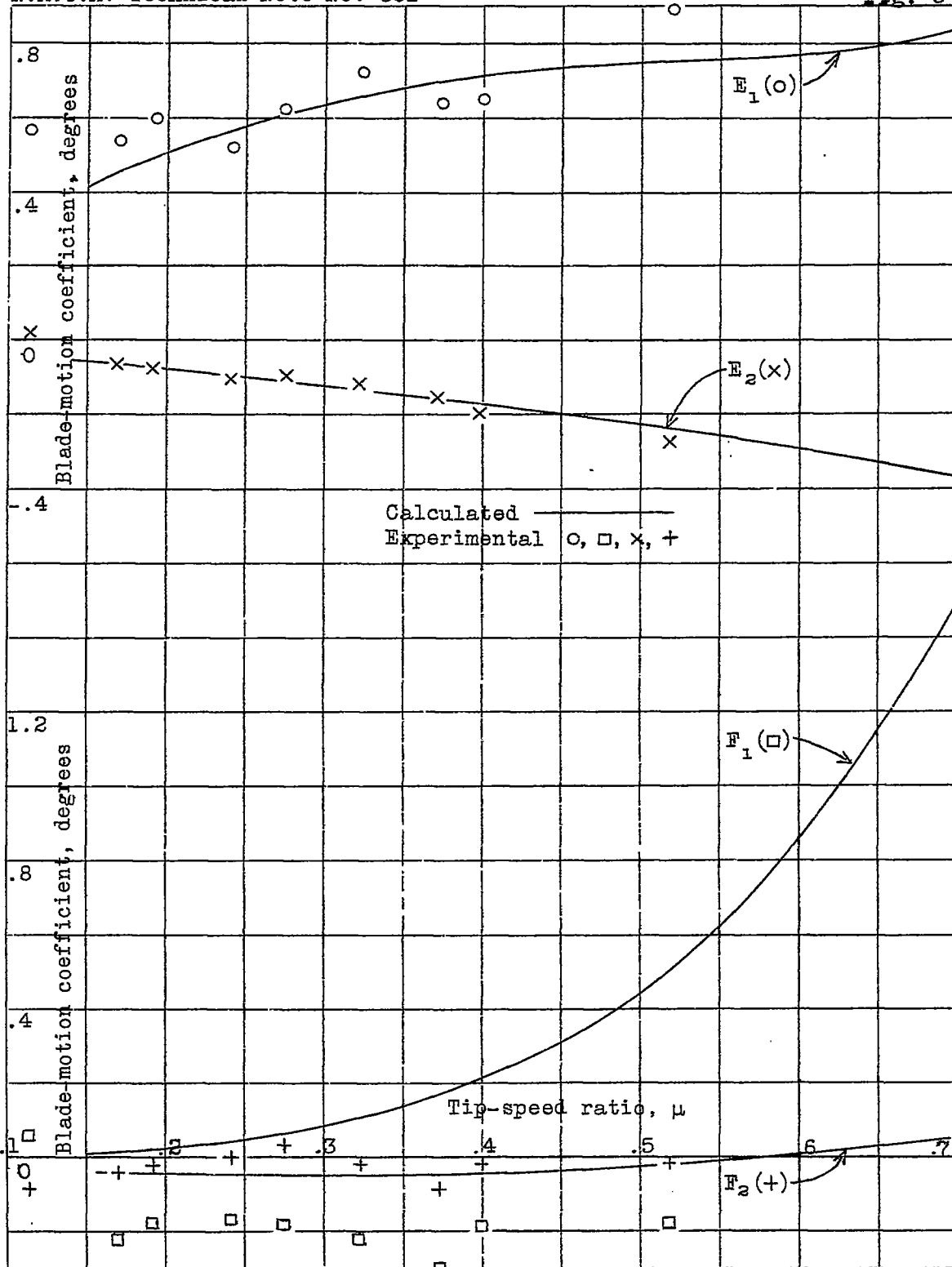


Figure 5.- Coefficients of PCA-2 rotor-blade motion about the vertical pin as measured in flight and as calculated from the air forces and the angular momentum.

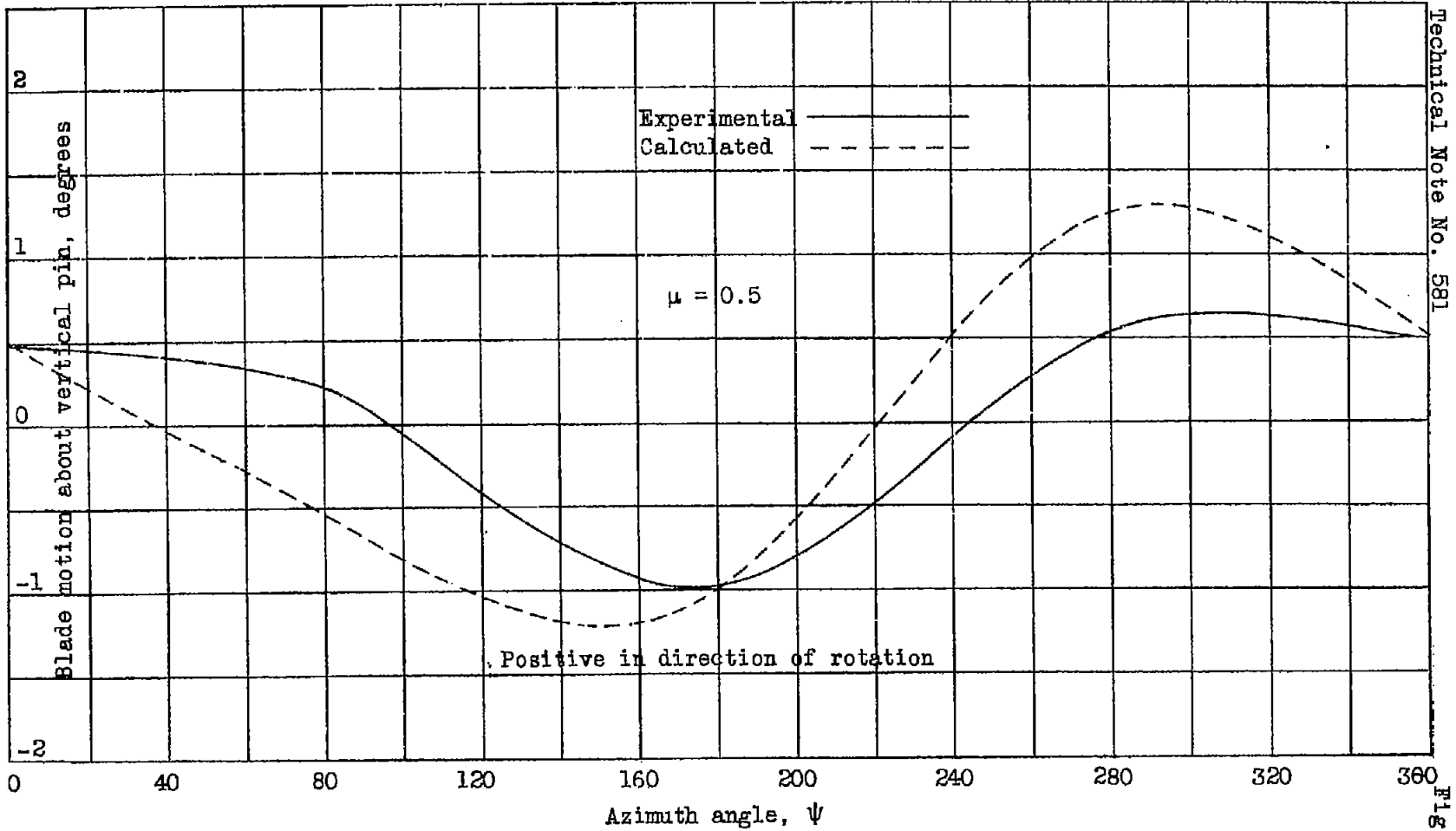


Figure 6.- PCA-2 rotor-blade motion as measured in flight and as calculated from the angular momentum alone.

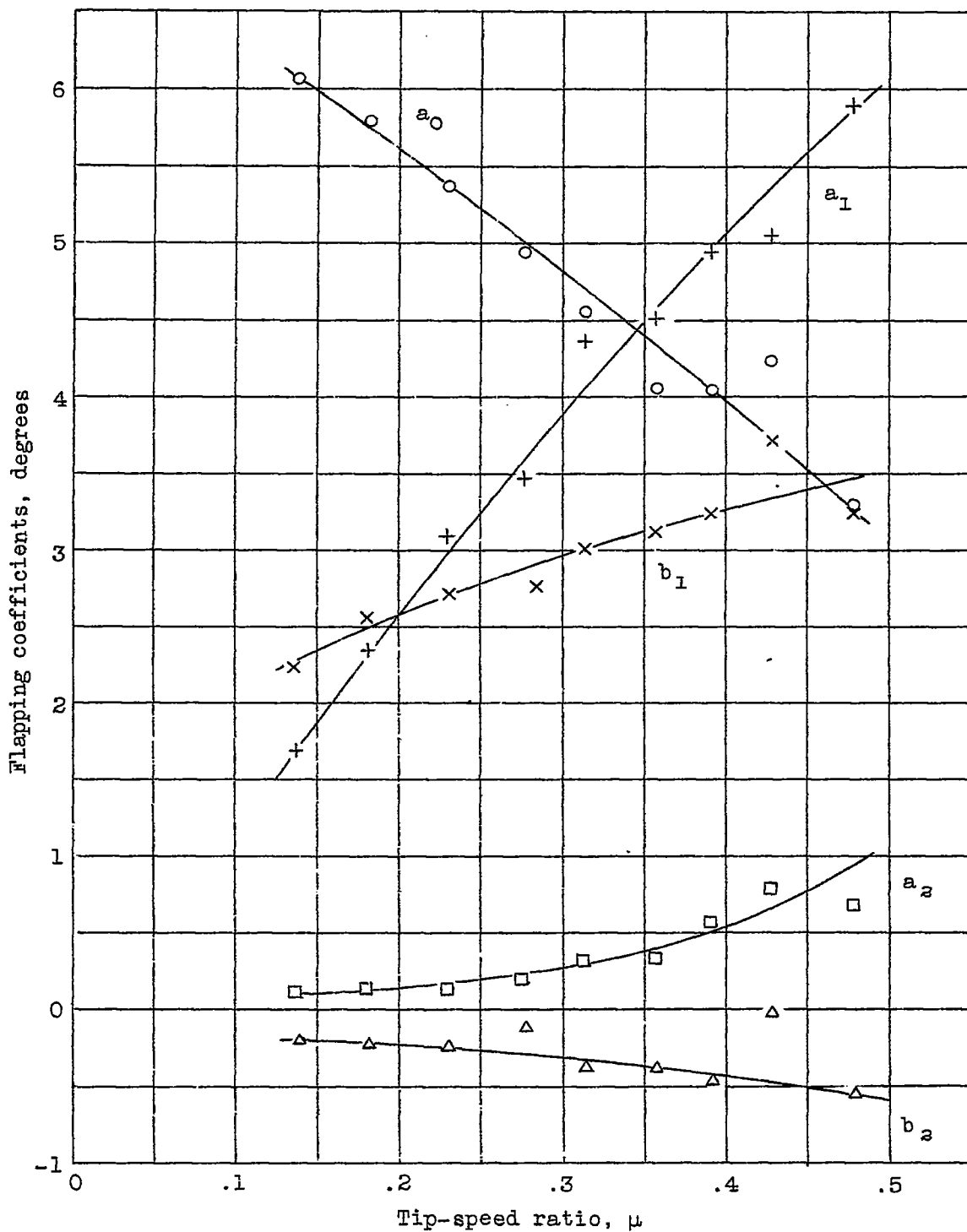


Figure 7.- Flapping coefficients of the PAA-1 autogiro rotor blade as measured in flight.

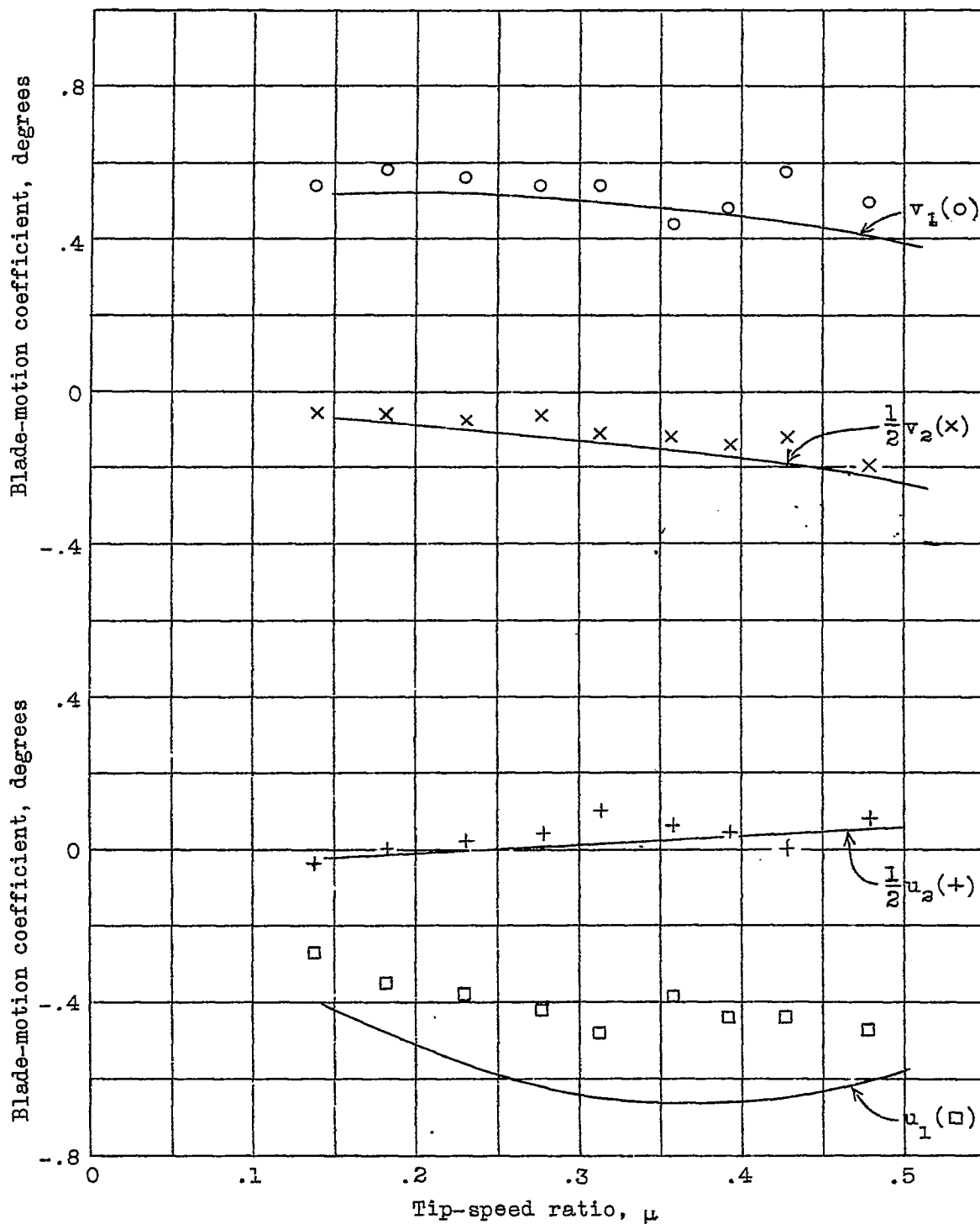


Figure 8.- Coefficients of the PAA-1 rotor-blade motion about the vertical pin as measured in flight and as calculated from the angular momentum alone.

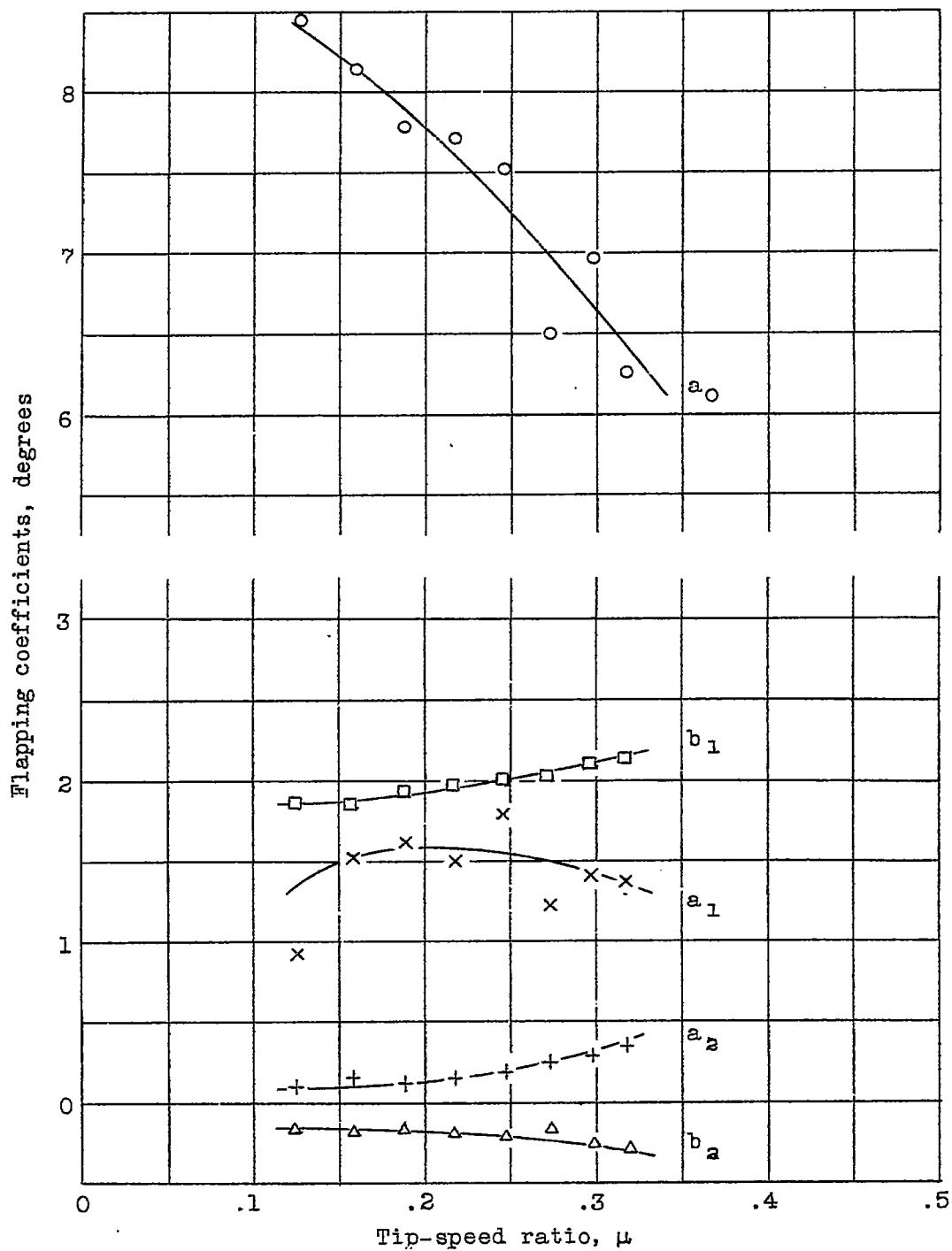


Figure 9.- Flapping coefficients of the KD-1 autogiro rotor blade as measured in flight.

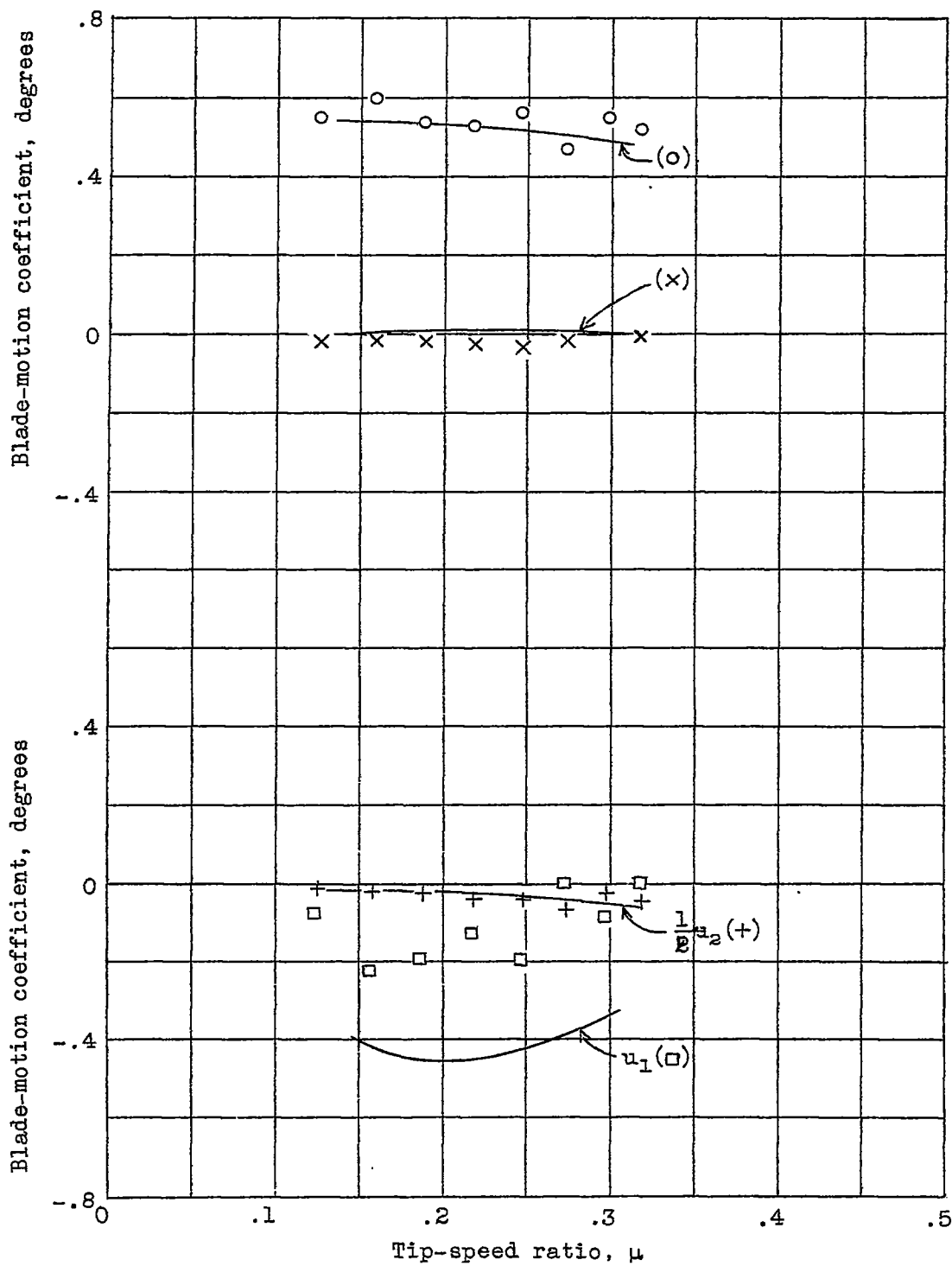


Figure 10.- Coefficients of the KD-1 rotor-blade motion about the vertical pin as measured in flight and as calculated from the angular momentum alone.